Virtual Calibration Chamber CPT on Ticino sand

J. Butlanska, M. Arroyo & A. Gens
Department of Geotechnical Engineering, UPC, Barcelona, Spain

ABSTRACT: The following paper summarizes results of CPT's performed in virtual calibration chamber (VCC) built with a 3D model based on the distinct element method (DEM). A discrete material tailored to mimic Ticino sand is tested at different densities, stress and stress history. The limit cone tip resistance from the numerical experiments shows quantitative agreement with different empirical curves summarizing previous tests on Ticino sand in physical calibration chambers (ENEL and ISMES).

1 INTRODUCTION

The cone penetration test (CPT) remains to this day one of the major devices for geotechnical site characterization. While interpretation of the test results in clay has advanced considerably from the theoretical and numerical point of view that of tests in sand still relays largely on empirical correlations. A major source of such correlations is done in calibration chambers (CC), where soil state and properties can be controlled.

Arroyo et al (2009) describe in detail how a virtual calibration chamber (VCC) might be built using a three-dimensional model based on the discrete element method (DEM). Results from physical tests in Ticino sand (Jamiolkowski et al. 2003) were employed to check the proposed procedure. It was shown that under isotropic confinement stresses and boundary conditions of the BC1 type (σ_v = const, σ_r = const) the VCC results were in good quantitative agreement with the predictions of the empirical equations based on the physical tests.

In this paper, after recalling some previous results, further numerical experiments using the VCC are presented. The methodology is applied again to Ticino sand but, this time, under non-isotropic confinement and using both BC1 and BC3 (σ_v = const, $\varepsilon_r = 0$) boundary conditions. Also the influence of the CPT rate of penetration is explored through a specific test series.

2 METHODOLOGY

2.1 *Numerical method*

The PFC3D code developed by ITASCA was used to perform all simulations mentioned in this paper. The code follows closely the discrete element method introduced by Cundall & Strack (1979). The model is composed of distinct particles that displace independently of one another, and interact only at the contact or interfaces between particles. The particles are assumed rigid with no ability to rotate. The contact law employed is lineal elasto – plastic. The normal and tangential stiffness at any contact, k_n and k_s, are described by the following scaling rule:

$$k_N = 2K_{eff}\frac{D_1 D_2}{D_1 + D_2} \qquad (1)$$

$$k_S = \alpha k_N$$

where K_{eff} , α = parameters to be calibrated. The plastic part of the contact law is given by the interparticle friction angle, $\Phi\mu$. No cohesion was included in the contact model. Our simulations also employed non–viscous damping, δ, to achieve rapid convergence.

2.2 *Model calibration*

The numerical model used for calibration was designed as a small cubical sample with side of 8 mm, contained 4700 particles with the grain size curve showed in Figure 1 (DEM curve-fitted). The specimen was built to specified porosity using radius expansion method (REM, Itasca 2005).

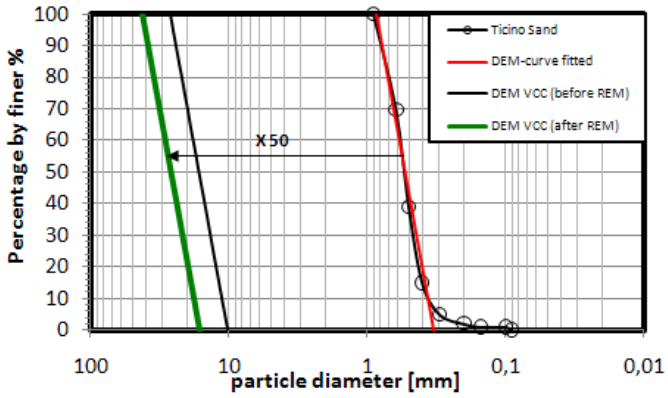

Figure 1. Grain size distribution of Ticino sand and DEM models

The material parameters that require calibration are only interparticle friction (Φ_μ), those related to stiffness (K_{eff}, α) and damping (δ). These parameters were determined by trial and error in order to provide a best fit to a single isotropically compressed drained triaxial test (TEST M09) confined at 100 kPa and formed with D_R = 75%. The best fit was found with parameters: K_{eff} = 300 MN, α = 0.25, δ = 0.05 and μ = 0.35 (equivalent to an interparticle friction angle, Φ_μ=19.3º). The adequacy of these calibration parameters was verified by simulating a variety of triaxial tests at differing confinement and initial density (Arroyo et al. 2009).

2.3 *VCC CPT*

The cone angle is 60º and is modelled as perfectly rough. The cone shaft is described with four successive rigid cylindrical walls, which first three of them (h = 0.1 m each) are frictional and the last one frictionless. Sleeve friction was measured only as the friction against the first frictional segment. The geometry of the numerical calibration chamber (VCC) is cylindrical, given by its height H and diameter D_{cc}. Dimensional analysis of the problem (Arroyo et al., 2009) quickly reveals that an unmanageably large number of particles are needed if the VCC tries to mimic the physical tests.

Table 1. Summary of geometrical characteristics of CC

Dimension	Units	physical CC	numerical VCC
Dcc	[m]	1.2	1.2
Hcc	[m]	1.5	0.7

Numerical constraints thus required a certain reduction in chamber height (Table 1). More importantly, they also required scaling up the mean grain size. The material filling the virtual chamber was a scaled Ticino Sand where grain size was multiplied 50 times to achieve a manageable number of particles. This resulted in 65,000 elements in the densest specimens, almost an order of magnitude more than the number employed in previous 2D studies (Ma 1994, Calvetti & Nova 2005 and Jiang et al. 2006). The grain size curve of the material in the VCC is shown in Figure 1 (DEM VCC (after REM)).

Several sizes of cone tip were employed; however most of the penetration tests were performed with cone tip of 71.2 mm in diameter. That is double the cone diameter used in the experimental calibration chamber tests (35.6 mm). The ratio (R_d) between calibration chamber (D_{cc}) and cone diameter (d_c) in those conditions is 16.8.

2.4 *Testing program*

Results from three tests series are presented in the following. The main test series (Series I, for details see Arroyo et al. 2009) was performed under BC1 boundary conditions, and examined relative densities of 75% and 90% under initial isotropic stresses ranging from 60 to 400 kPa. The second series, (Series II) was performed on dense samples (D_R > 90 %) at different stress states after anisotropic consolidation (K_0-conditions) under two different boundary conditions (BC1 & BC3). The third series (Series III) was performed with the specific aim of exploring the influence of penetration rate on the test results.

The boundary condition nomenclature here employed is that usual when discussing CC tests: BC1 means a test where all the stress components are constant during penetration; BC3 means a test where vertical stress is kept constant and no radial deformation is allowed during penetration.

3 RESULTS

3.1 *Raw results and data processing*

The cone penetration tip resistance curves recorded for test Series I can be seen in Figure 2a. As expected, the cone tip resistance increases with confining pressure and relative density. However, the graphs are quite noisy, with large oscillations. The steady

state observed in the experimental CC research was not easily observed in the numerical simulations. That numerical noise, however, can be filtered out easily. To do that, a steady state cone resistance is extracted from the raw penetration curves by fitting them to the following expression:

$$q_c(h) = a \cdot (1 - e^{-b \cdot h}) \qquad (2)$$

where a = steady state cone resistance ($q_{c,lim}$); b = fitting parameter; h = penetration depth; and q_c = recorded cone tip resistance. A graphical example of the curve fit for the extraction of limit cone resistance can be seen in Figure 2b.

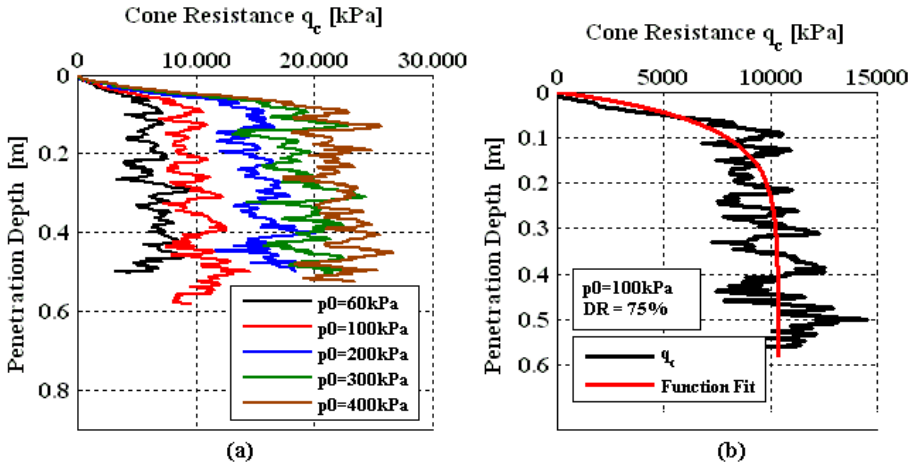

Figure 2. Raw cone penetration resistance curves from test Series I: (a) tests with target D_R = 75% and (b) example of curve-fit for the extraction of limit cone resistance, Series I, p_0=100kPa, D_R=75%.

The main reason for the oscillatory noise in the numerical curves is the reduced cone diameter to mean particle size ratio, ($n_p = d_c / D_{50}$). In the tests here discussed n_p is just 2.7, a value necessary to achieve manageable computations. Simulations with increasing cone diameter in a fixed chamber size (Arroyo et al, 2009) show that a $n_p \approx 8$ already results in a very smooth penetration curve.

Just as in physical calibration chambers, a chamber size-effect needs to be accounted for. For the BC1 tests here performed we use a correction factor, CF, based on Jamiolkowski et al. (2003):

$$CF = a\left(D_R\right)^b$$
$$a = 9 \cdot 10^{-5} R_d^{2.02} \qquad (3)$$
$$b = -0.565 \ln\left(R_d\right) + 2.59$$

The correction factor depends on the cone diameter ratio, ($R_d = D_c / d_c$). Here R_d =16.8 in all the numerical tests presented. For tests performed under BC3 conditions no correction factor is applied.

3.2 *Series I: comparison with existing empirical correlations*

Jamiolkowski et al. (2003), using results from CPT tests on normally and overconsolidated physical samples of Ticino sand, proposed the following Schmertmann-type empirical correlation:

$$q_{c,ref} = C_0 \cdot p_a \cdot \left(\frac{p'}{p_a} \right)^{C_1} \cdot e^{C_2 \cdot D_R} \qquad (4)$$

where p_a = is the atmospheric pressure, D_R = relative density and p' = is mean effective stress. For Ticino sand, the authors quoted propose $C_0 = 23.19$, $C_1 = 0.56$ and $C_2 = 2.97$. The numerical results in test Series I have no direct physical counterpart, since they were performed after isotropic consolidation and not after K_0 consolidation. However, the numerical result, corrected for calibration camber size effect, can be compared with the prediction given when the corresponding relative density and mean stress of the test are input into equation (4). The results can be seen on Figure 3, where a rather good agreement is observed.

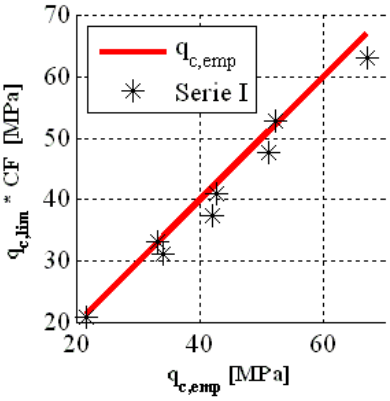

Figure 3. Comparison of corrected cone resistance from isotropically confined DEM tests and the predictions of the empirical correlation obtained for Ticino sand Eq. 4.

3.3 *Series II: comparison with tests on a physical CC*

The numerical results of series II correspond to CPT tests performed after anisotropic consolidation (K_0 conditions) in the VCC. The initial conditions before CPT are collected in Table 2. These tests allow for a more direct comparison with physical CC results; indeed, Table 2 presents a list of numerical and physical tests from the ENEL/ISMES database. Differences between a numerical test and its counterpart in relative density are within 2%; those in stress are slightly higher (within 15%, averaging 8%), but, according to equation (4) carry less weight.

Table 2. Summary of the numerical tests in Series II and their physical counterparts

TEST ID (num/exp)	BC [-]	OCR [.]	D_R [%] (num/exp)	σ_v [kPa]	σ_r [kPa] (num/exp)	$q_{c,lim}/q_{c,exp}$ [MPa] (num/exp)	q_c*DEM/q_c*CC [MPa] corrected for CF
NUM1/T140	1	1	93.9/92.62	121,6	48.69/54.1	6.495/18.7	16.31/32.18
NUM2/T161	1	1	93.9/95.53	212.1	78.69/88.3	10.291/26.4	25.84/45.65
NUM3/T163	1	1	96.8/95.82	313.0	109.91/132.7	13.037/32.3	33.75/56.10
NUM4/T141	3	1	93.9/92.52	121,6	48.69/53.2	24.440/22.6	25.41/22.57
NUM5/T162	3	1	93.9/95.53	212.1	78.69/89.9	35.410/29.3	35.41/29.28
NUM6/T164	3	1	96.8/95.47	313.0	109.91/132.3	40.797/34.6	40.80/34.57
NUM7/T160	1	3.396	93.4/94.97	62.3	38.05/46.1	5.872/16.6	14.66/28.20
NUM8/T148	3	3.545	93.4/93.78	62.3	38.05/46.3	18.519/16.7	18.52/16.68
NUM9/T77	3	2.800	90.8/90.85	113.7	61.55/83.4	24.324/26.2	24.32/26.20

Typical comparisons between the numerical cone penetration curves and their physical correlates are shown in Figure 4. The results from tests under BC3 conditions can be compared directly with their physical counterparts, since there is no calibration chamber size correction to be applied. A fair agreement is observed (Figure 4b). On the other hand, tests under BC1 conditions need to be corrected for chamber size effects and the correction is different for the numerical tests (with R_d =16.8) and the physical tests (where R_d = 33.7). As shown in Figure 4a there is a sizeable discrepancy between the corrected numerical and physical results, although, perhaps haphazardly, the corrected numerical result falls on top of the uncorrected physical curve.

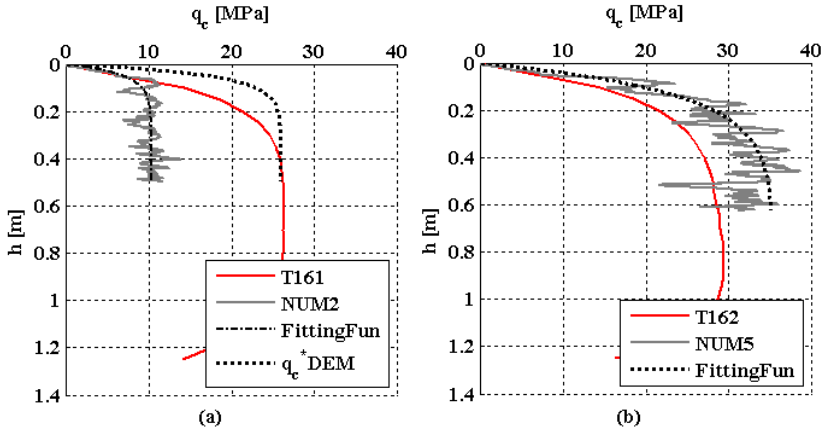

Figure 4. DEM VCC cone penetration curves and physical parallel tests on Ticino sand (a) test T161 BC1 (b) test T162 BC3

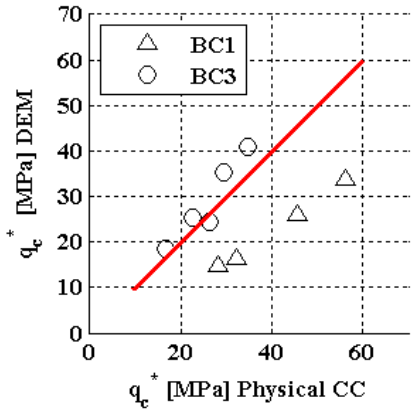

Figure 5. Comparison of corrected cone resistance from DEM VCC CPT (Series II) and physical parallel tests on Ticino sand

The results just commented are typical for all tests in Series II. As shown in Figure 5, there is a striking difference in behavior between the numerical tests performed under BC3 conditions which compare fairly well with the physical counterparts and those performed under BC1 conditions, which give corrected cone resistances 50-60% of those corresponding to their physical counterparts.

3.4 *Influence of velocity rate on CPT*

In the physical CC the penetrometer was normally inserted into the ground at 20mm/sec. However, it is numerically convenient to increase the penetration rate, while still ensuring that inertia effects are second order. To explore this issue a parametric analysis including seven velocity rates in the range from 20 to 500mm/sec was performed. The numerical model was prepared under one dimensional compression with σ_v = 121.6 kPa and K_0 = 0.400, e_0 = 0.611. The penetration was performed under BC1 boundary conditions. It was observed, (Figure 6), that penetration rate had a very minor effect on the cone penetration resistance. The mean value was 6.29 MPa and the standard deviation of 0.13. Apart form this series all the other numerical simulations here presented have been performed with a penetration rate of 100 mm/sec.

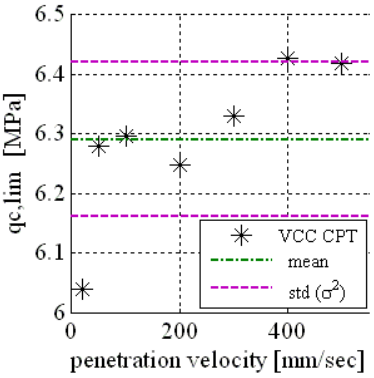

Figure 6.Influence of penetration velocity on cone resistance.

4 DISCUSSION

Series I included some tests performed at high relative density (above 90%) that are directly comparable (except for the different consolidation procedure employed) with the BC1 tests in Series II. When the numerical results (corrected for size effect) are plotted against the prediction of the physically based correlation (equation 4) the behaviour of the isotropically consolidated samples is clearly better than that of the anisotropically consolidated ones (Figure 7). This seems to exclude as a cause of systematic error the fact that the CC size effect correction factor has been extrapolated into a lower range than that for which it was developed.

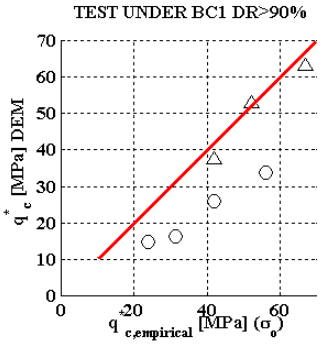

Figure 7. Comparison of virtual BC1 tests on dense Ticino sand with the empirical predictions for isotropically consolidated samples (Series I) and anisotropically consolidated samples (Series II)

It is not clear at this stage why tests performed under BC1 conditions after anisotropic consolidation are performing worst than both BC1 tests after isotropic consolidation and BC3 tests after anisotropic consolidation. A possibility currently being explored relates to the numerical implementation of the change in lateral boundary condition between that prevailing in anisotropic consolidation (zero radial strain) and the BC1 (constant radial stress).

5 CONCLUSION

To the best of our knowledge these are the first reported three-dimensional DEM - based simulations of CPT. The quantitative agreement generally obtained with physical experiments represents a remarkable improvement with respect to previous attempts, whose 2D nature made a quantitative comparison difficult. Such agreement was obtained despite the simplification in particle shape and size distribution, behaviour and model construction that were required to obtain practical results using a standard-capacity PC. It is clear that (a) the methodology here applied would likely need some extensions to address other sands, particularly those for which grain crushing is important (b) some improvement in the implementation of boundary conditions BC1 after anisotropic consolidation is necessary. However, our results suggest that by correcting for the unavoidable differences of scale, it is possible to use the DEM method to simulate successfully the results of cone penetration tests performed in a calibration chamber under controlled conditions.

REFERENCE

Arroyo, M. Butlanska, J., Gens, A.., Calvetti, F. & Jamiolkowski, M. 2009. Cone penetration tests in a virtual calibration chamber (under review)

Butlanska, J., Arroyo, M. & Gens, A. 2009. Homogeneity and symmetry in DEM models of cone penetration, *Powders & Grains, Vol. I*

Calvetti, F. & Nova, R. 2005. Micro-macro relationship from DEM simulated element and in-situ tests. *Powders & Grains, Vol. I, pp. 1292-1299*

Cundall, P.A. & Strach,O.D.L. 1979. A discrete numerical model for granular assemblies. *Geotechnique, vol.29, No.1, pp.47-65*

Garizio, G.M.. 1997. Determinazione dei parametric geotecnici e in particolare di Ko da prove penetrometriche, *M.Sc. Thesis*

Jamiolkowski, M., Lo Presti, D.C.F. & Manassero, M. 2003. Evaluation of relative density and shear strength of sands from CPT and DMT, in *Germaine, Sheahan & Whitman, Soil Behavior and soft ground construction, ASCE Geotechnical Special Publication 119, 201-238*

Jiang, M.J., Yu, H-S & Harris, D. 2006. Discrete element modelling of deep penetration in granular soils. *Int. J. Numer. Anal. Meth. Geomech. vol.30, pp. 335-361*

Ma, M.Y.1994. A numerical study of cone penetration test in granular assemblies. PhD Thesis. Clarkson University.